



NASA Technical Memorandum 81904

NASA-TM-81904 19810003934

DEPLOYABLE AND ERECTABLE CONCEPTS FOR LARGE SPACECRAFT

H. G. Bush, W. L. Heard, Jr., J. E. Walz and J. J. Rehder

OCTOBER 1980

LIBRARY COPY

NOV 14 1980

LANGLEY RESEARCH CENTER
LIBRARY, NASA
HAMPTON, VIRGINIA

NASA

National Aeronautics and
Space Administration

Langley Research Center
Hampton, Virginia 23665

FOR REFERENCE

NOT TO BE TAKEN FROM THIS ROOM

ABSTRACT

Computerized structural sizing techniques are used to determine structural proportions of minimum mass tetrahedral truss platforms designed for low earth and geosynchronous orbit. Optimum (minimum mass) deployable and erectable, hexagonal shaped spacecraft are sized to satisfy multiple design requirements and constraints. Features integrated into the sizing procedure include design for: 1) packaging constraints imposed by Space Shuttle limits, 2) fundamental vibration frequencies of the platform and struts, 3) strut axial stiffness reduction due to curvature and/or taper, 4) strut buckling due to design loads such as gravity gradient control, orbital transfer, or assembly, and 5) geometric constraints on strut thickness, diameter and length. Strut dimensions characterizing minimum mass designs are found to be significantly more slender than those conventionally used for structural applications. Comparison studies show that mass characteristics of deployable and erectable platforms are approximately equal and that the Shuttle flights required by deployable trusses become excessive above certain critical stiffness values. Recent investigations of erectable strut assembly are reviewed. Initial erectable structure assembly experiments show that a pair of astronauts can achieve EVA assembly times of 2-5 min/strut and studies indicate that an automated assembler can achieve times of less than 1 min/strut for around the clock operation.

INTRODUCTION

The aerospace community faces a major challenge in the future to devise ways to accomplish missions currently being considered. These missions involve spacecraft sizes which range from state-of-the-art antennae to futuristic, kilometer-class solar power satellites. The extremely high cost of transporting mass to orbit, even with Space Shuttle, dictates that maximum efforts be made to minimize mass carried into space. Little information exists, however, to define efficient proportions to characterize the structures required by future large spacecraft. Structural proportions can severely affect packaging and as a consequence, the number of Space Shuttle flights required to transport the spacecraft to low earth orbit.

Previous studies identified low-mass trusses as a candidate structural class which meets the requirements of many future missions. These studies examined trusses which are deployable (unfolded on-orbit^{1,2}), erectable (assembled on-orbit³⁻⁸), and space fabricated (manufactured and assembled on-orbit⁸⁻¹⁰) and are characterized by a large number of design variables (structural dimensions) and requirements. Due to the absence of a computerized sizing procedure with sufficient generality to integrate the necessary design requirements and system constraints into the design process, sizing activities in these investigations are limited. Instead, the major effort previously has been to determine the adequacy of conservatively sized spacecraft structures to meet mission requirements.

The purpose of this paper is to determine trends in Space Shuttle transportation and mass characteristics of efficiently proportioned large space platforms. Both deployable and erectable spacecraft, with their unique constraints, are examined. Sensitivity studies are performed to illustrate the impact of key parameters on efficient designs. Also, preliminary results of assembly studies for erectable structures are presented and assessed.

N81-12445 #

ANALYTICAL APPROACH

Computerized Structural Sizing

The determination of structural sizes and proportions which satisfy specified design requirements can be accomplished many ways. The requirement that these structural dimensions be "optimum" in some sense increases the complexity of the design process. The efficient determination of optimum dimensions for structural systems of unusual configurations or with a large number of design variables, requires the use of computerized optimization techniques. This technology is well developed and is currently being used to find solutions for a variety of problems such as designing control systems for aircraft and ships, improving ride quality for automobiles, performing aircraft aerodynamic wing design, and sizing structural components. A schematic diagram of the structural sizing approach for platforms used herein is shown in figure 1. The desired platform geometry is specified in terms of the sizing variables (dimensions). Analyses of the various design requirements are considered simultaneously (instead of sequentially) by the optimizer. The optimization routine involves mathematical programming techniques that determine structural dimensions which simultaneously satisfy the requirements and optimize a specified function, such as mass, cost, etc.. Although many satisfactory techniques are available, the constrained minimization (CONMIN) method¹¹ is used in this study.

Platform Geometry

A tetrahedral truss platform is selected for study due to its low mass and high stiffness characteristics². This platform, shown in figure 2(a), has a hexagonal planform. The face and core struts can be dissimilar if required by the sizing process; however, all struts are made of graphite-epoxy material with properties given in Table 1. Both deployable and erectable truss platforms are sized for transport to orbit via Space Shuttle. The deployable platform is unfolded on-orbit while the erectable platform is assembled on-orbit. Transportation of either platform type imposes unique constraints on the structural sizing process through the way each concept packages in the Space Shuttle cargo bay.

Deployable platform packaging. The deployable platform is considered to be constructed of cylindrical struts as shown in figure 2(b). The platform is considered to have inward folding face struts; therefore, the face struts can never be longer than the core struts. The core struts have an upper limit on length, which is taken to be 18 m (slightly less than the Shuttle cargo bay length). A hexagonal-shaped tetrahedral platform folds into a hexagonal-shaped package with the arrangement shown in figure 2(b). The cross-sectional area of this package is a function of the strut diameter, d . The cluster joint radius required for parallel and compact strut stowage is shown in figure 2(b) and is:

$$r_{cl} = \frac{d_f + \sqrt{3(3d_f + 2d_c)} (d_f + 2d_c)}{4} \quad (1)$$

where subscripts f and c refer to face and core struts, respectively. The center-to-center spacing, S, of the cluster joints in the folded configuration is:

$$S = 2r_{cl} + d_f \quad (2)$$

The maximum diameter of the hexagonal-shaped package, d_p , and the area of this package, A_p are:

$$d_p = \frac{SD}{\ell_f} \quad (3)$$

$$A_p = \frac{3\sqrt{3}}{8} d_p^2 \quad (4)$$

where D is the maximum span of the deployed hexagonal platform shown in figure 2(a). The maximum allowable value of d_p per Shuttle flight is 4.27 m, which is slightly less than the diameter of the Shuttle cargo bay. Therefore, on a cross-sectional area basis, the number of Shuttle flights required to transport a given platform can be approximated as:

$$SF = \frac{A_p}{A_{cb}} = \frac{3\sqrt{3}}{2\pi} \left(\frac{d_p}{4.27\text{m}} \right)^2 \quad (5)$$

where A_{cb} is the useable cross-sectional area of the Shuttle cargo bay. On a mass basis, the number of Shuttle flights required is:

$$SF = \frac{M_{sys}}{29480 \text{ kg}} \quad (6)$$

where 29480 kg is the total payload capability of Space Shuttle. A minimum estimate of the Shuttle flights required to transport a given platform to low earth orbit is given by the maximum value of either equations (5) or (6). The problem of joining segments of a deployable truss when multiple Shuttle flights are required is not addressed in this study.

Erectable platform packaging. The erectable platform truss is constructed of tapered, nestable struts which are packaged in Shuttle in stacks of strut halves, as shown in figure 2(c). The stacks of strut-halves may not exceed 18 m in length. The stacking increment, Δ , shown in figure 2(c) is:

$$\Delta = \frac{t}{d} \frac{1+\lambda}{1-\lambda} \sqrt{d^2 \left(\frac{1-\lambda}{1+\lambda} \right)^2 + \left(\frac{\ell}{2} \right)^2} \quad (7)$$

where $\bar{d} = (d_1 + d_2)/2$ and $\lambda = d_1/d_2$. Subscripts 1 and 2 denote minimum and maximum strut diameters, respectively.

The number of strut halves per stack is:

$$N = \frac{18m - (\ell/2)}{\Delta} + 1 \quad (8)$$

All variables in equations (7) and (8) must be subscripted with either an f or c to denote face or core strut values, respectively. A square packing array is considered for the cross-sectional arrangement of the stacks. Maximum diameters of the face and core struts, d_2 , determine the cross-sectional area, A_p , required for stowage of the erectable platform, which is:

$$A_p = \frac{2n_f d_{2f}^2}{N_f} + \frac{2n_c d_{2c}^2}{N_c} \quad (9)$$

where the number of face struts, $n_f = 3(D/\ell_f)^2$

and the number of core struts, $n_c = 1.5(D/\ell_f)^2$

On a cross-sectional area basis, the number of Shuttle flights may be approximated from equation (9) as:

$$SF = \frac{A_p}{A_{cb}} = \frac{4A_p}{\pi (4.27m)^2} \quad (10)$$

On a mass basis, the Shuttle flights required by an erectable truss are also given by equation (6). Therefore, an estimate of the Shuttle flights required by a given erectable truss is given by the maximum value of either equation (10) or (6).

Optimized Function. The function selected for optimization (minimization) in this study is truss mass per unit area:

$$\frac{M}{A} = \frac{4\sqrt{3}\rho_f A_f \ell_f}{\ell_f^2} + \frac{2\sqrt{3}\rho_c A_c \ell_c}{\ell_f^2} + \frac{M_j}{A} \quad (11)$$

where the strut cross-sectional areas, A_f and A_c , are average values for nestable struts, ρ is the material density, and M_j is the total mass of all joints.

Sizing Variables. The structural dimensions (sizing variables) used in this study and their practical limits are:

Sizing Variable	Face Struts	Core Struts	Sizing Variable Limits
wall thickness	t_f	t_c	$\geq .508 \text{ mm}$
diameter	d_f	d_c	(deploy.)
	d_{1f}	d_{1c}	(erect.)
	d_{2f}	d_{2c}	
length	l_f	l_c	$\leq 18 \text{ m (deploy.)}$ $\leq 36 \text{ m (erect.)}$

Design Constraints. Each design requirement considered requires an analytical relation (or analysis) from which structural response is calculated. A summary of analytical relations used in this study is presented in the Appendix. These design requirement analyses are used to form inequality relations which the truss is constrained to satisfy. The design requirements considered and corresponding constraints used in this study are:

Design Consideration	Constraint
f_T , Truss Fundamental Frequency (free edges)	$f_T \geq f_d$
f_s , Strut Fundamental Frequency (simply supported)	$f_s \geq k f_d$
P , Strut Load (simply supported)	$P \leq P_E$

where: f_d = platform design frequency (specified)
 k = strut design frequency factor (specified)
 P = P_d (ass'y, docking, maneuvering, etc., load--specified)
 \quad = P_{gg} (gravity gradient load)
 \quad = P_{ot} (orbital transfer load)
and P_E = Strut Euler buckling load

Other structural effects considered which impact the truss design are initial strut curvature (deployable and erectable) and strut taper (erectable). Strut curvature can result from a manufacturing imperfection, from lateral acceleration during maneuvering in space, or from thermal bowing of the strut on-orbit. Both curvature and taper reduce the strut axial stiffness (see equations (A7) and (A10)), and consequently, the overall bending stiffness of the truss.

RESULTS AND DISCUSSION

Low Earth Orbit Platforms

The structural mass per unit area and Shuttle flight requirements of spacecraft for low earth orbit (LEO) application are examined. Numerical results for both deployable and erectable spacecraft with spans of 400 m and 800 m are presented. The sensitivity of minimum mass designs to variations in selected parameters is investigated to identify areas of high payoff (i.e., key design drivers) which would benefit from further study. Strut and platform vibration frequencies are calculated in this study considering strut loads to be zero.

Platform Design Frequency. The effect of the platform design fundamental frequency, f_d , (a measure of platform stiffness) on structural mass per unit area and Shuttle flights is shown in figure 3 for three platform sizes. These calculations were made assuming straight struts, a strut frequency factor, $f_s/f_d = 10$ (to prevent coupling from occurring between platform and strut modes) and a distributed non-structural mass, $m_p = 0.1 \text{ kg/m}^2$, which is representative of a low mass reflector surface.

The structural mass per unit area is shown by the lower family of curves in figure 3. Deployable (dashed lines) and erectable (solid lines) platforms are shown to have equivalent masses at lower values of design frequency (on the order of reflector mesh surfaces) because of minimum gage and minimum strut diameter limits. Mass per unit area is shown to increase rapidly for higher values of design frequency (stiffness). The increased structural mass necessary to meet higher stiffness requirements is accentuated by platform size, as seen by comparing the 800 m results with the smaller platforms.

The strong impact of platform design frequency (stiffness) on transportation is shown in figure 3 by the Shuttle flights (upper family of curves) required to transport the various platforms to LEO. For lower values of design frequency, the Shuttle flights required by deployables and erectables are equivalent, as shown by the horizontal portions of the curves. Shuttle flights in this region are governed by mass considerations, and not the geometry or packaged size of the structures, which are different for each type of platform. At higher values of platform frequency (stiffness), the deployable platform strut dimensions are sufficiently large that package size dominate the Shuttle payload and the curves become nearly vertical. The Shuttle flights required by erectable platforms exhibit a more gradual increase, being controlled by the minimum mass requirements. Thus, for a given size platform, nestable struts permit use of a stiffer structure without incurring transportation inefficiencies, than possible with deployable platforms. Different design requirements will not alter this result; they will only change the frequency (stiffness) at which the deployable limit occurs.

The effect of platform design frequency on minimum mass strut proportions is illustrated in figure 4 for an 800 m deployable platform. At lower frequencies strut wall thickness and diameter are at lower bounds and the lengths of both face and core struts decrease with increasing design frequency. This result occurs because strut frequency, and not platform frequency is controlling the design in this region ($f_T > f_d$), and truss depth must increase to meet higher stiffness requirements, until the maximum strut length of 18 m is reached. For greater frequencies, the higher platform bending stiffness can no longer be obtained by increasing platform depth (core strut length), hence the face struts must become thicker, larger in diameter, and shorter to supply the required platform bending stiffness.

Structural proportions which characterize minimum mass designs are important. Strut slenderness ratios (length-to-radius of gyration) calculated from the data in figure 4 vary from approximately 500 at the higher platform frequencies to approximately 4000 at the lower platform frequencies. Conventional slender tubes are usually limited to slenderness values of less than 200¹. Thus, fabrication of structural platforms using struts with non-conventional slenderness ratios may require advanced manufacturing techniques to insure strut straightness and length control.

Strut Frequency. Calculations presented in figures 3 and 4 were made assuming a strut design frequency factor, $f_s/f_d = 10$. The effect of varying f_s/f_d is presented in figure 5. Results are shown for erectable and deployable platforms for both 400 m and 800 m spans. The mass per unit area requirements at the strut frequency factor of 10 is approximately 4-5 times greater than at a factor of 2. The Shuttle flights required by the 400 m platforms considered here are not adversely affected by the strut frequency factor. However, an abrupt increase in Shuttle flights occurs for the 800 m deployable platform above a strut frequency factor of 5, indicating that a practical limit of this parameter probably exists for other large size deployable platforms or smaller platforms with more severe design requirements.

Strut Curvature. Strut curvature is defined as the ratio of initial lateral displacement at the center of the strut to the strut length, δ/ℓ . The effect of curvature is to reduce the axial stiffness of the face struts (eq. (A7)) and thus reduce the bending stiffness of the platform (eqs. (A1) and (A2)). Consider the 800 m and 400 m deployable platforms with perfect struts, and $f_d = .1$ Hz shown in figure 3. A vibrational analysis of these designs, for various strut curvatures is shown in figure 6. The resulting frequency of the truss with curved struts, f_T , is 18% and 36% lower than the value with straight struts, f_d , for the 800 m and 400 m platforms, respectively, at a strut curvature of $\delta/\ell = .001$. This value of initial strut curvature is at the lower boundary of the range conventionally recommended for design purposes¹². Larger values of initial strut curvature lead to even greater reductions in the truss fundamental frequencies as shown in figure 6. However, as shown in figure 7 (upper curves), sizing for this initial curvature will maintain the .1 Hz design frequency with only a small increase in structural mass up to $\delta/\ell = .001$. Beyond this point, both structural mass per unit area and Shuttle flights for the deployable platform increase abruptly.

For the 400 m deployable platform with $\delta/\ell = 0$, struts are minimum gage and the Shuttle flights are controlled by mass considerations. Increasing strut curvature has little effect as long as minimum gage and minimum diameter struts

are sufficient to meet design criteria. However, when strut dimensions exceed minimum limits sufficiently for Shuttle flights to become volume controlled, transportation requirements increase dramatically. The results for erectable platforms shown in figure 7 do not exhibit any abrupt increases. However, similar to the deployable platform, the erectable strut proportions vary markedly with increased strut curvature.

Strut Design Load. For the platforms studied herein, strut loads induced by gravity gradient control were insignificant. However, other loads such as result from docking, maneuvering, or assembly loads for erectable platforms could be significant. The effect of a constant strut design load is shown in figure 8. Shuttle transportation for the erectable platforms is relatively unaffected over the load range considered. The impact of strut design load on the Shuttle transportation for the 400 m deployable platform is significant, increasing from one-half flight, for essentially zero design load, to approximately four flights for a design load of 400 N. The increased strut cross-section required for the higher loads causes a packaging penalty which is reflected in the Shuttle transportation requirements for the 400 m deployable platform. The 800 m deployable platform Shuttle transportation requirements indicate that the larger strut cross-sections required to satisfy frequency constraints are sufficient to carry strut loads up to approximately 100 N. Above this value, strut cross-section increases significantly to carry the load, as shown by the increased Shuttle flight requirements.

Distributed Payload. Previous calculations were performed for an assumed membrane reflector type distributed mass. Figure 9 shows the structural mass per unit area and Shuttle transportation requirements for variations in this parameter ranging from membrane reflector, $m_p \approx .1 \text{ kg/m}^2$, to solar collector, $m_p \approx 1 \text{ kg/m}^2$, (cells) type surfaces. As can be seen, structural mass of the 400 m platform is not greatly affected for either deployable or erectable structure. A factor of 20 increase in the distributed payload mass results only in approximately a 30% to 40% increase in structural mass per unit area. Transportation requirements for both the 400 m deployable and erectable platforms are mass controlled and increase nearly proportionally to the increase in distributed payload mass. The mass per unit area of the 800 m platforms is similar until the deployable platform depth becomes constrained by the core strut length of 18 m at $m_p \approx .3 \text{ kg/m}^2$. For larger values of m_p the increased stiffness required to meet the specified design frequency, cannot be achieved as efficiently with the deployable platforms as with an erectable structure. Consequently, for a payload of 2 kg/m^2 the structural mass per unit area for the 800 m deployable platform is twice as great as that for the corresponding erectable platform. The ratio of the structural mass to the total mass for all platforms considered is approximately 40%-50% for a payload of $.1 \text{ kg/m}^2$ but decreases to 8%-15% for a payload of 2 kg/m^2 .

Geosynchronous Orbit Platforms

The design of spacecraft for geosynchronous orbit (GEO) application must consider additional requirements not imposed on LEO spacecraft. One requirement, which has substantial impact on spacecraft sizing and design, is the orbital transfer maneuver. Although not absolutely necessary, it is

desirable to deploy or assemble large spacecraft in LEO, near Space Shuttle, so that man can provide any maintenance or servicing required before transferring the spacecraft to GEO in its functional state. Chemical propulsion is currently being examined¹³ as a method for transferring the spacecraft. This poses problems by introducing large, discrete thrust loads (relative to ion or electric propulsion) into a large skeletal truss framework.

An initial assessment of structural loads resulting from transferring minimum mass platforms from LEO to GEO is made. The effect of such loads on platform structural mass per unit area and Shuttle flight requirements is examined. These studies are limited to considering only constant thrust chemical propulsion systems and deployable platforms. The availability of a given thrust level engine is not considered. Instead, an estimate of the required thrust for various size platforms is made based on minimum mass structural sizing results. Using the orbital transfer vehicle sizing capability^{13,14}, the propulsion system mass required to transfer a given spacecraft from LEO to GEO is determined for initial values of thrust-to-weight ratio, T/W_0 , of .001 through .1 and a wide range of spacecraft masses, and is shown in figure 10. This propulsion system information is incorporated into the structural sizing procedure.

The propulsion system thrust load is applied normal to the tetrahedral truss back-face at three nodal hard points located symmetrically about the center of gravity of the hexagonal planform truss as shown in figure 11. Eq. (A5) gives the load induced in those core struts which transmit the applied thrust into the surrounding structure. Comparison of eq. (A5) with finite element analyses indicates that maximum strut load for the cases examined is accurately predicted. Although strut loads decay away from the thrust application points, this decay is not considered herein and all struts are designed to carry the maximum load, given by eq. (A5).

Using this approach, deployable platforms of 100 m, 150 m, and 200 m spans are sized for $T/W_0 = .001$, .01, and .1. Results for the minimized structural mass per unit area and Shuttle flight requirements of the platform are shown in figure 12. (Shuttle transportation requirements for the propulsion system are not shown). For the conditions specified, these results indicate the maximum size platform that could be placed in GEO, using one Shuttle flight to LEO, is approximately 200 m, for $T/W_0 = .01$. If faster orbital transfer times are required, multiple Shuttle flights are required for a 200 m deployable platform. System requirements not considered here, such as the volume and mass requirements of attitude control systems, electrical power or control system data distribution wiring, or thermal control insulation will further reduce the transportability of the deployable platforms shown in figure 12.

The maximum strut loads which result from the orbital transfer maneuver are shown in figure 13 as a function of T/W_0 for three platform sizes. Strut loads are shown to increase rapidly with T/W_0 . An estimate of the total constant thrust required to accomplish orbital transfer of the platforms is also shown in figure 13. Total thrust requirements vary from 100 N to 300 N at $T/W_0 = .001$ and from 1000 N to 3000 N at $T/W_0 = .01$.

ERECTABLE PLATFORM ASSEMBLY

Astronaut Assembly

For those applications where folding platforms, complete with functional equipment and systems, cannot be efficiently transported or reliably deployed, erectable structures, characterized by nestable struts appear to offer an alternative. However, erectable spacecraft must be assembled on orbit--an operation which appears formidable when first considered. Many currently perceived potential near term missions require spacecraft of 100 to 300 m span¹⁵. While large by present spacecraft standards, such structures can involve hundreds--not thousands-- of structural components placing them potentially within the capability of astronaut assembly. Since Man's capability for assembling structural components in a weightless, pressure suited environment is virtually unexplored a series of tests was undertaken at the NASA Marshall Space Flight Center Neutral Buoyancy Facility. These initial experiments investigated the capability of two pressure suited astronauts to assemble a six-strut tetrahedral cell shown in figure 14, using various strut lengths, joint hardware, and assembly procedures. The average unassisted assembly times for various pairs of subjects is shown in figure 15. The bounding lines around the data indicate the general learning curve trend. As more tests were conducted, experience was gained and the assembly times decreased, appearing to approach approximately five min/strut for the unassisted assembly tests shown. Other tests employing different approaches yielded assembly times of approximately two min/strut, illustrating the usefulness of assembly aids for improving astronaut efficiency in performing weightless assembly tasks. The NBF tests thus far provide needed qualitative information on specific task performance by pressure suited astronauts. Future experiments must investigate ways to enhance and maintain astronaut productivity over longer periods of time than studied previously.

Automated Assembly

Some proposed missions require erectable spacecraft sufficiently large or complex (in a system sense) that astronaut capability is more efficiently used performing tasks other than structural assembly. For such spacecraft, it would be desirable to automate the assembly process as much as possible. A preferred concept has emerged from studies¹⁵ and is artistically depicted in figure 16 in a free flying mode assembling a large platform. A detailed sketch of this automated assembler is shown in figure 17. Conceptually, the machine is an assemblage of simple mechanisms which perform specific sequential operations to construct repetitive truss structures, either linear beams or area platforms, using nestable struts.

The assembler consists of two pairs of swing arms, each pair connected by a tie-rod and a gimballed four-sided main frame. Cannisters, containing nested half-struts and/or nodal joints are attached to the arm and frame members. In the platform assembly mode, the machine operates by alternately swinging the upper and lower arms to walk from node-to-node (hardpoints) along the platform edge inserting struts and nodes which are dispensed from the cannisters as it progresses. Strut halves are snapped together as the machine steps, using a strut assembly mechanism, an early example of which is shown in the figure. This machine can also operate in a beam assembly mode, assembling struts as

explained previously to build a linear structure in a direction perpendicular to the assembler main frame, as shown in figure 17. Whether or not the assembler operates as a free flyer or remains Shuttle attached must be determined from assembly dynamics and control studies.

Theoretically, such an automated machine is capable of assembly rates of less than one min/strut and can operate around the clock, requiring astronaut involvement only for surveillance, maintenance or servicing. The capability of this automated general purpose machine to perform installation of other spacecraft systems along with the structure assembly process is currently being examined to further increase its versatility and utility.

Assembly Assessment

A preliminary perspective of assembly capability may be drawn from the studies to date. The on-orbit assembly time required to construct platforms of 100 m to 1000 m span, using 20 m nestable struts is shown in figure 18 for various assembly rates. The simulated EVA assembly rates are derived using NBF data for one pair of astronauts, and assuming that these rates are applicable for 8 hrs/day, not necessarily performed all in one shift or by the same people. The automated machine assembly rates are derived using the theoretical timelines and assuming 24 hr/day operation.

It is shown in figure 18 that within the five-day on-orbit operational limit of Space Shuttle, approximately a 200 m span platform could be assembled by astronauts. It is also shown that a much larger platform, on the order of 400-500 m span, could be erected with the automated assembler in the same five-day time period. Conversely, the machine is also applicable to more rapid construction of smaller platforms or beams to reduce astronaut structural assembly tasks, or free them for systems installation and checkout duties.

Viewing the results shown in figure 18 in a qualitative, rather than quantitative sense, indicates that both man and machine can make significant contributions, either independently or together, toward assembling spacecraft on-orbit. The level of involvement using either method is an issue which requires much future study, and then will probably be decided on a case-by-case basis.

CONCLUDING REMARKS

Ultra-low mass designs of large deployable and erectable tetrahedral truss platforms which meet a variety of practical requirements and constraints are identified using computerized structural sizing (mathematical programming) techniques. These designs are characterized by structural mass per unit area which is equivalent to that of mesh reflector surfaces. Platform fundamental frequency, which is a measure of overall structural stiffness, is shown to be a strong design driver, indicating a need to determine the minimum acceptable value of this parameter which will permit mission accomplishment.

Strut proportions characterizing minimum mass designs of deployable and erectable trusses are found to be much more slender than struts conventionally used for earthbound structural applications. The axial stiffness of these slender minimum mass struts, and consequently the platform bending stiffness (frequency) is shown to be extremely sensitive to curvature of the strut axis. This situation indicates a need to include in the sizing procedure, strut

curvature from all sources, such as manufacturing, gravity effects, thermal bowing, or lateral acceleration due to orbital transfer and maneuvering. If the full advantages of minimum mass, slender strut construction are to be realized, a fabrication capability for long thin-walled, small diameter, straight, filamentary composite tubes--both cylindrical and tapered-- must be developed.

For platforms with minimum stiffness requirements, optimum deployable and erectable structures were found to require approximately the same number of Shuttle flights for transporting to orbit. Higher platform stiffness requirements or more severe design constraints, however, result in increased strut diameters which significantly increases the Shuttle flights required by deployable structures and limits their usefulness. Erectable platforms were found not to be limited in this manner because of the more efficient packaging of nestable struts, thereby offering an alternative for platforms with stiffness requirements that cannot be efficiently met by deployable structure.

In general, strut stiffness requirements were found to impact deployable structures more severely than erectable structures primarily due to the resultant increase in Shuttle flights required. The severe effect on structural proportions of maintaining high strut frequency relative to platform frequency indicates a need to determine the minimum value of this parameter required to prevent vibrational coupling between strut and platform.

Preliminary structural sizing calculations, considering transfer to GEO using chemical propulsion with initial accelerations of .01 g or less, indicate that up to a 200 m deployable platform may be transported to LEO with a single Shuttle flight.

An initial assessment of astronaut assembly (100 struts/day) of erectable struts, indicates that approximately a 200 m hexagonal platform could be assembled within the operational constraint of one Shuttle flight using an astronaut pair in EVA. Automated assembly was found to permit faster assembly (1 strut/min.), reduction in astronaut activity, or the construction of larger platforms within the same time period.

APPENDIX

The following equations summarize the structural design relations used in this study. These equations are applicable to a hexagonal platform, tetrahedral truss structure with dissimilar face and core struts. Pertinent design equations are presented for both deployable (cylindrical strut) and erectable (nestable strut) construction. Derivations of these and relations for other platforms are presented in references 3, 5, 6, and 17.

Platform Equations

The platform bending stiffness is given as:

$$D_T = \frac{3\sqrt{3}}{8} E_f A_f \ell_f \left[\left(\frac{\ell_c}{\ell_f} \right)^2 - \frac{1}{3} \right] \quad (A1)$$

which assumes that the platform may be idealized as a sandwich plate with isotropic face sheets and a rigid core.

The platform fundamental frequency may be expressed in terms of equation (A1) as:

$$f_T = \frac{25.93}{2\pi D^2} \sqrt{\frac{D_T g_\xi}{(M/A)_{sys}}} \quad (A2)$$

where $(M/A)_{sys}$ is the total system mass per unit area and includes strut mass, joint mass, and payload mass. All system mass is assumed to be uniformly distributed. The constant g_ξ is defined as:

$$g_\xi = 1 \frac{\text{kg} \cdot \text{m}}{\text{N} \cdot \text{s}^2} = 32.2 \frac{\text{lb}_m \cdot \text{ft}}{\text{lb}_f \cdot \text{s}^2} \quad (A3)$$

The constant, 25.93, was determined from a finite element vibrational analysis of a hexagonal plate.

The gravity gradient load in the face struts is most critical when the struts are aligned in the direction of loading⁵ and may be expressed as:

$$P_{gg} = \frac{15\sqrt{3}}{256} \frac{g_0}{g_\xi} \frac{R_e^2}{R^3} \frac{(M/A)_{sys} D^3}{\sqrt{\left(\frac{l_c}{l_f}\right)^2 - \frac{1}{3}}} \left[1 - \frac{1}{2} \left(\frac{M_c}{M_{sys}} + \frac{2M_f}{M_{sys}} \right) \right] \quad (A4)$$

where M_{sys} is the total system mass including all strut, joint, and payload masses, R is the orbit radius measured from the center of the earth, R_e is the Earth's radius, and g_0 is the Earth's gravitational acceleration.

The orbital transfer load is a maximum in the core struts shown in figure 10 for the cases considered in this study. Application of the orbit transfer thrust load at three nodal points located symmetrically about the platform mass center results in:

$$P_{ot} = \frac{1}{6} \frac{l_c}{\sqrt{l_c^2 - \frac{1}{3} l_f^2}} \frac{T}{W_0} \frac{M_0}{M_{sys}} M_{sys} g_0 \left(\frac{1}{1 + M_{dry}/M_{sys}} \right) \quad (A5)$$

where T is the thrust, M_{dry} is the mass other than the platform structure and payload that remains at the end of the apogee burn, and W_0 is the startburn weight referenced to the Earth's surface. The ratio of startburn mass, M_0 , to system mass, and the ratio of dry mass to system mass is obtained as a function of T/W_0 from interpolation of data produced by the system of computer programs AVID12,13.

Cylindrical Strut Equations

The strut fundamental frequency, assuming simply supported ends, may be approximated as:

$$f_s = \frac{\pi}{2\ell^2} \sqrt{\frac{g_\xi EI(1 - P/P_E)}{\left(\rho A + \frac{\pi M_{Cj}}{48 \ell}\right)}} \quad (A6)$$

where M_{Cj} is the appropriate center joint mass. Other parameters in eq. (A6) are the strut mass density ρ , material modulus E , length ℓ , cross-sectional area A and moment of inertia I . The quantity g_ξ is defined in equation (A3).

The strut extensional stiffness for initially curved struts can be approximated as:

$$\frac{(EA)_{\text{curved}}}{(EA)_{\text{straight}}} = \left[\frac{1}{1 + \frac{8}{15} \left(\frac{\delta}{r_g}\right)^2 \left(\frac{1}{1 - P/P_E}\right)^3} \right] \quad (A7)$$

where δ is the initial lateral deflection at the center of the curved strut, r_g is the strut radius of gyration, and P is the strut load.

Nestable Strut Equations

The strut fundamental frequency for a nestable strut, assuming simply supported ends, may be approximated as:

$$f_s(\text{nest.}) = C f_s(\text{cyl.}) \quad (A8)$$

where $C = f(d_1/d_2) = 1.08$ for $.4 \leq d_1/d_2 \leq .5$. The term $f_s(\text{cyl.})$ is computed from equation (A6) using average values for the nestable strut cross-sectional area and moment of inertia.

The strut Euler buckling load may be expressed as:

$$P_E = \frac{mEI_2}{\ell^2} \quad (A9)$$

where I_2 is the maximum moment of inertia of the strut cross-section. The factor m is given as a function of the minimum-to-maximum diameter ratio of the strut.

The strut extensional stiffness can be expressed as a function of the minimum-to-maximum diameters of the strut⁷. The result is:

$$\frac{(EA)_{\text{nestable}}}{\overline{EA}} = \frac{2(1 - \lambda)}{(1 + \lambda) \ln\left(\frac{1}{\lambda}\right)} \quad (A10)$$

where \overline{EA} is the extensional stiffness of an equal mass cylinder, and $\lambda = d_1/d_2$.

REFERENCES

- ¹ Armstrong, W. H., Skoumal, D. E., and Straayer, J. W., "Large Space Erectable Structures--Building Block Study," Final Report, NAS9-14914, Apr 1977.
- ² Barclay, D. L., et al., "Large Space Structures--Configuration, Packaging, and Response Studies," Final Report, NAS1-13967, Sep 1978.
- ³ Bush, H. G. and Mikulas, M. M., Jr., "A Nestable Tapered Column Concept for Large Space Structures," NASA TM X-73927, 1976.
- ⁴ Miller, K. H., "Solar Power Satellite Construction Concepts." Paper presented at the 23rd Annual Meeting of the American Astronautical Society's Industrialization of Space Conference, Oct 18-20, 1977.
- ⁵ Mikulas, M. M., Jr., Bush, H. G., and Card, M. F., "Structural Stiffness, Strength and Dynamic Characteristics of Large Tetrahedral Space Truss Structures," NASA TM X-74001, Mar 1979
- ⁶ Bush, H. G., Mikulas, M. M., Jr., and Heard, W. L., Jr., "Some Design Considerations for Large Space Structures," AIAA Journal, vol. 16, No. 4, Apr 1978, pp 352-359.
- ⁷ Heard, W. L., Jr., Bush, H. G., and Agranoff, N., "Buckling Tests of Structural Elements Applicable to Large Erectable Space Structures," NASA TM 78628, Oct 1978.
- ⁸ Nansen, R. H. and DiRamio, H., "Structures for Solar Power Satellites," Astronautics and Aeronautics, Oct 1978, pp. 55-59.
- ⁹ Browning, L., et al., "Space Construction Automated Fabrication Experiment Definition Study (SCAFEDS)," Final Report, Vol. II, NAS9-15310, May 1978.
- ¹⁰ Reinert, R. P., "Weight Optimization of Ultra Large Space Structures," Paper presented at the 38th Annual Conference of the Society of Allied Weight Engineers, Inc., May 1979.
- ¹¹ Vanderplaats, G. N., "CONMIN--A FORTRAN Program for Constrained Function Minimization--User's Manual," NASA TMX-62282, Aug 1973.

- 12 Timoshenko, S. P. and Gere, J. M., "Theory of Elastic Stability," 2nd Edition, McGraw Hill Book Company, 1961.
- 13 Rehder, J. J., and Wurster, K. E., "Electric vs. Chemical Propulsion for a Large-Cargo Orbit Transfer Vehicle," Journal of Spacecraft and Rockets, vol. 16, No. 3, May-Jun 1979, pp. 129-134.
- 14 Wilhite, A. W. and Rehder, J. J., "AVID: A Design System for Technology Studies of Advanced Transportation Concepts," AIAA Paper No. 79-0872, presented at the Conference on Advanced Technology for Future Space Systems, May 1979.
- 15 Jacquemin, G. C., Bluck, R. M., and Grotbeck, G. H., "Development of Assembly and Joint Concepts for Erectable Space Structures," NASA CR-3131, 1980.
- 16 Card, M. F. and Boyer, W. J., "Large Space Structures--Fantasies and Facts," AIAA Paper no. 80-0674 presented at the 21st Structures, Structural Dynamics and Materials Conference, May 12-14, 1980.
- 17 Heard, W. L., Jr., Bush, H. G., Walz, J. E., and Rehder, J. J., "Structural Sizing Considerations for Large Space Platforms," AIAA Paper No. 80-0680 presented at the 21st Structures, Structural Dynamics and Materials Conference, May 12-14, 1980.

Table I Graphite - epoxy material properties

	E_x	E_y	G_{xy}	ν_{xy}	α_x	α_y
	GPa	GPa	GPa		/K	/K
Uni-directional	131	10.9	6.4	.32	$-.54 \times 10^{-6}$	29×10^{-6}
Laminate (90.06/0.88/90.06)	117	25.4	6.4	.138	$.22 \times 10^{-6}$	11×10^{-6}

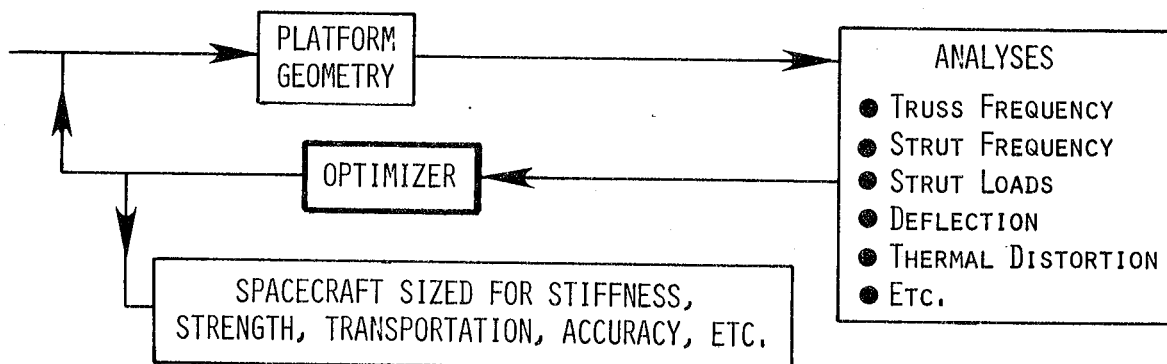


Figure 1. - Schematic diagram of optimization approach.

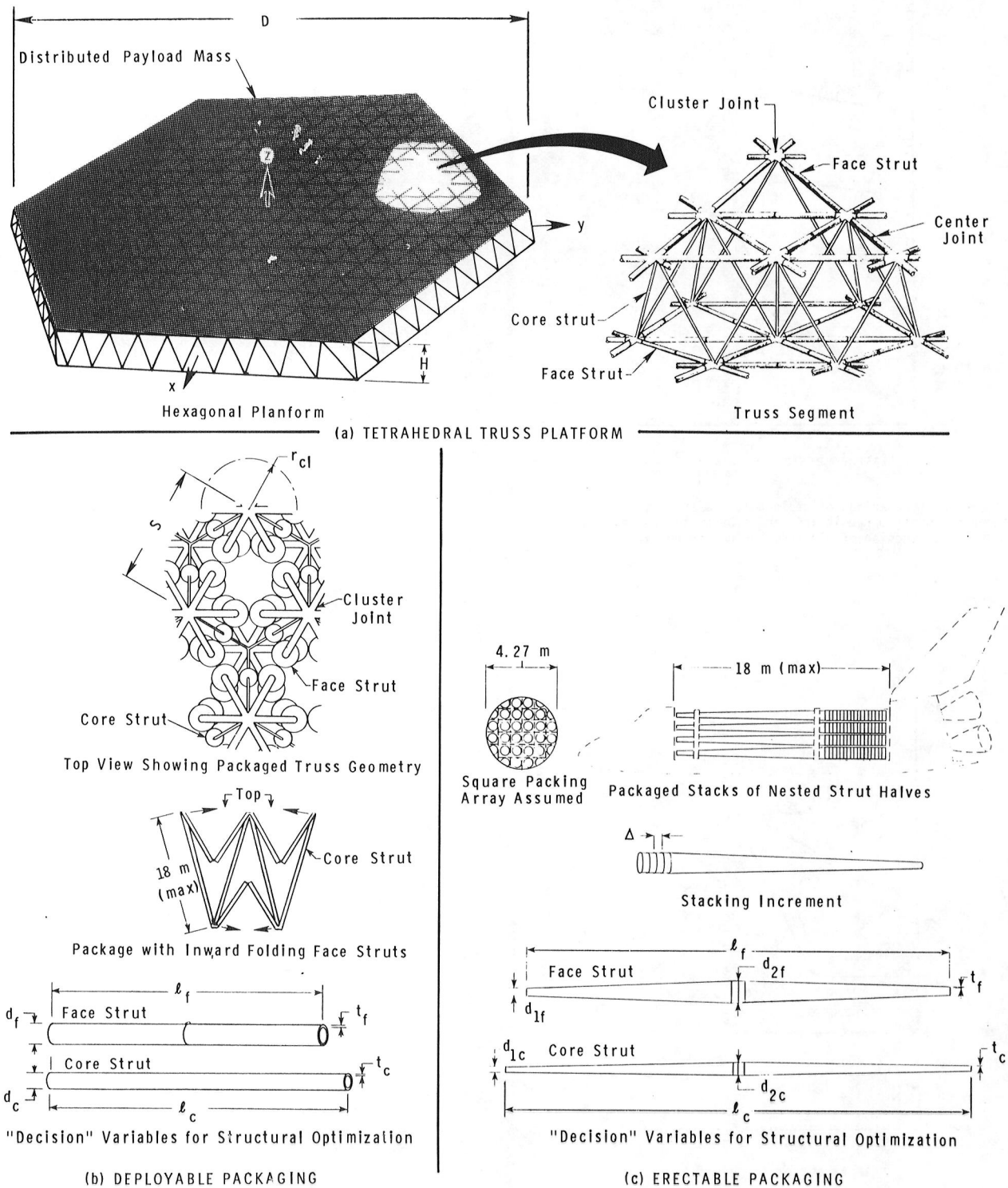


Figure 2. - Tetrahedral truss nomenclature and packaging geometry.

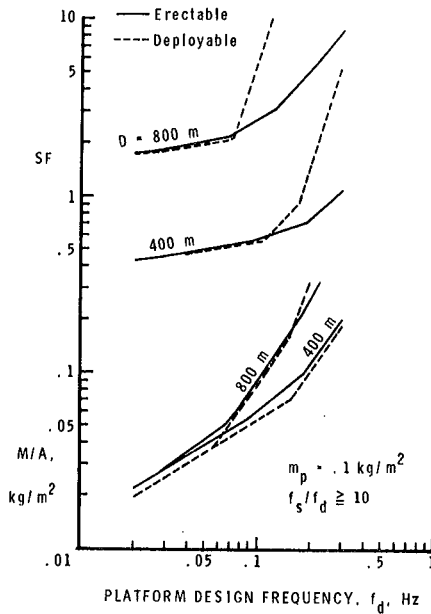


Figure 3. - Comparison of deployable and erectable platform structural mass per unit area and transportation requirements as a function of platform design frequency.

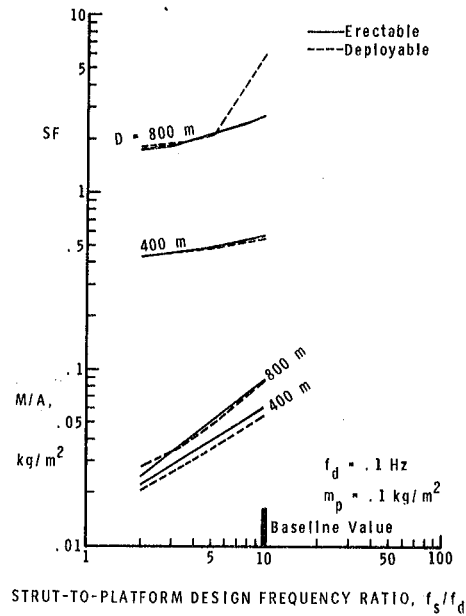


Figure 5. - Effect of strut-to-platform design frequency ratio on platform structural mass per unit area and transportation requirements.

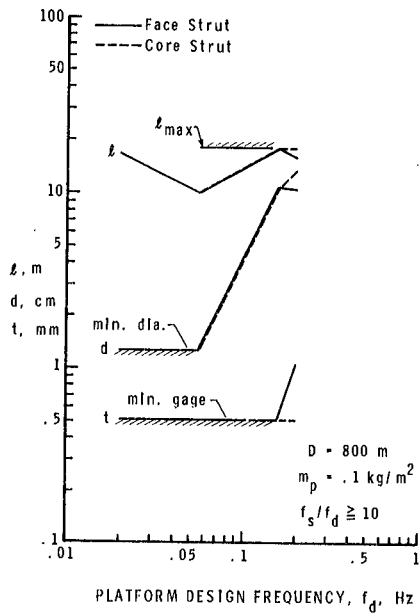


Figure 4. - Effect of platform design frequency on 800 m deployable platform strut geometry.

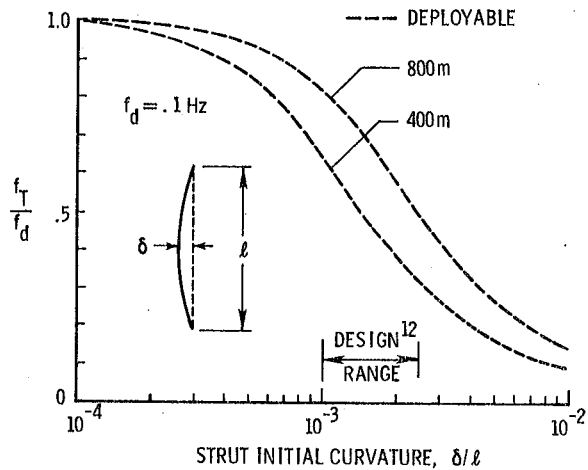


Figure 6. - Effects of strut initial curvature on platform fundamental frequency.

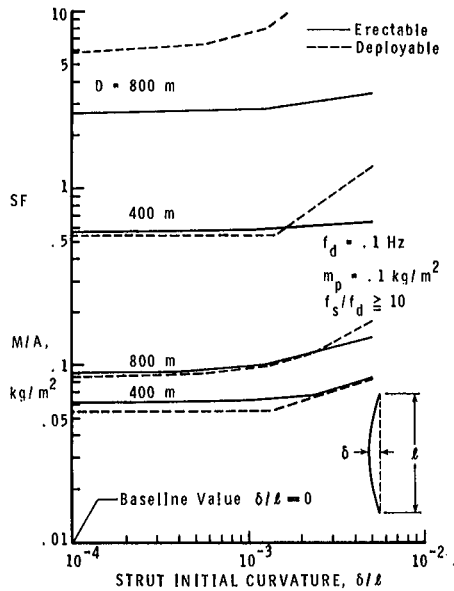


Figure 7. - Effect of strut initial curvature on platform structural mass per unit area and transportation requirements.

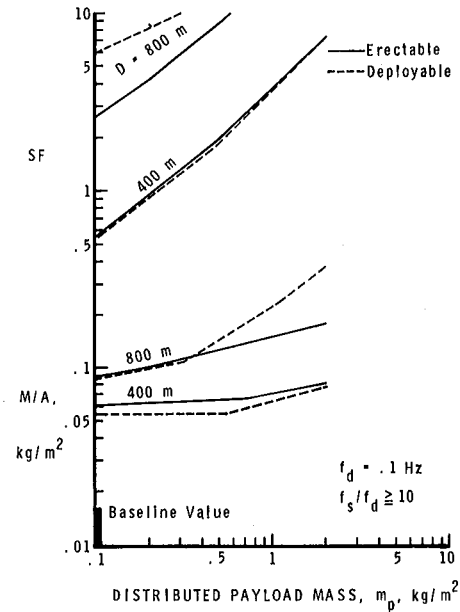


Figure 9. - Effect of distributed, non-structural (payload) mass on platform structural mass per unit area and transportation requirements.

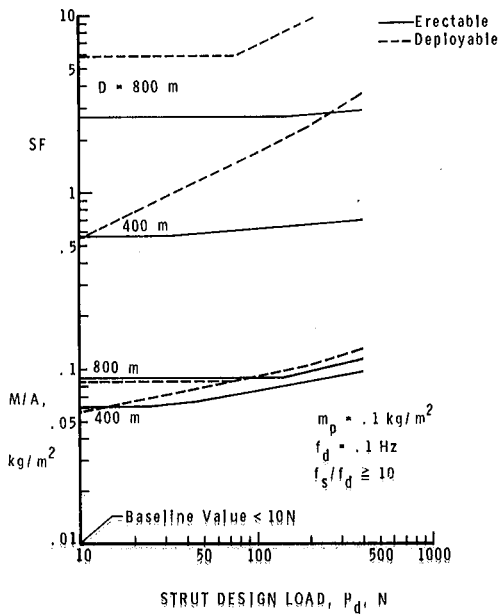


Figure 8. - Effect of strut design load on platform structural mass per unit area and transportation requirements.

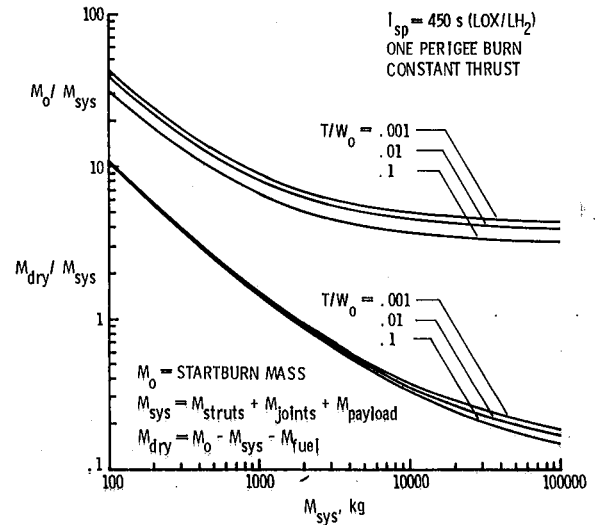


Figure 10. - Propulsion system mass characteristics required for LEO to GEO transfer as a function of spacecraft system mass.

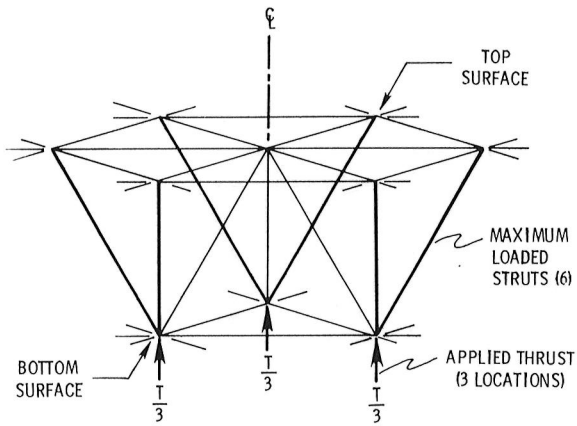


Figure 11. - Schematic of tetrahedral truss segment showing orbital transfer thrust load applied symmetrically around platform center.

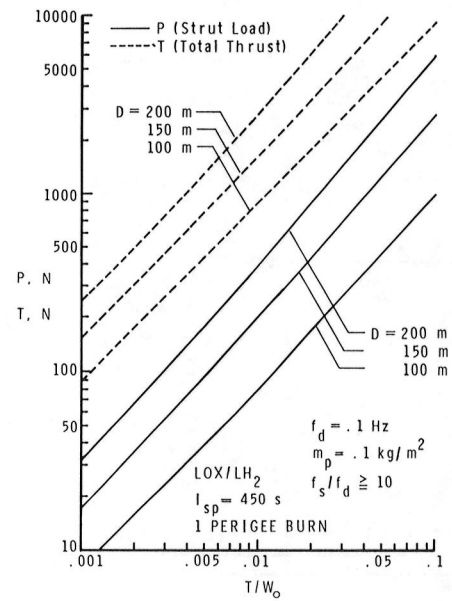


Figure 13. - Effect of thrust-to-weight ratio on total thrust required and on maximum core strut load for a deployable platform that is transported from LEO to GEO.

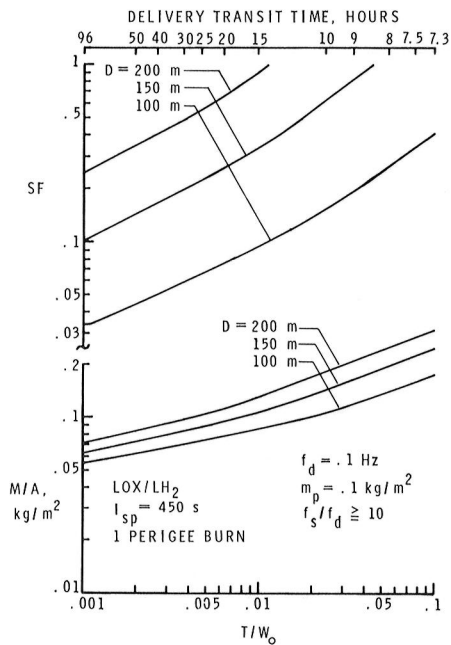


Figure 12. - Effect of thrust-to-weight ratio on structural mass per unit area and transportation requirements for a deployable platform that is transported from LEO to GEO.

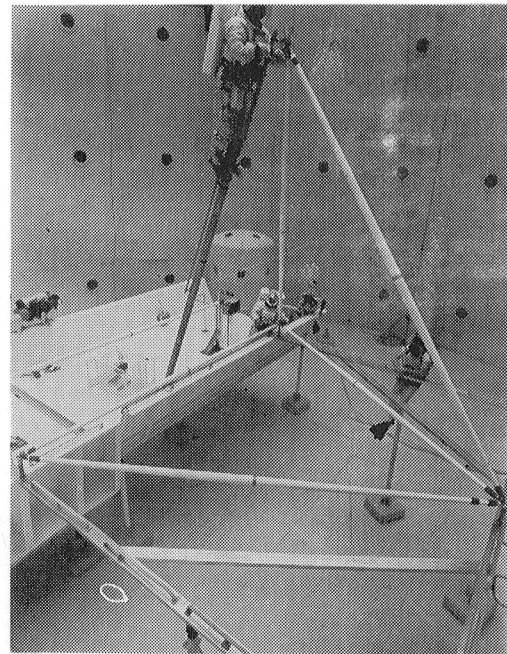


Figure 14. - Photograph of astronaut assembly experiment in Neutral Buoyancy Facility.

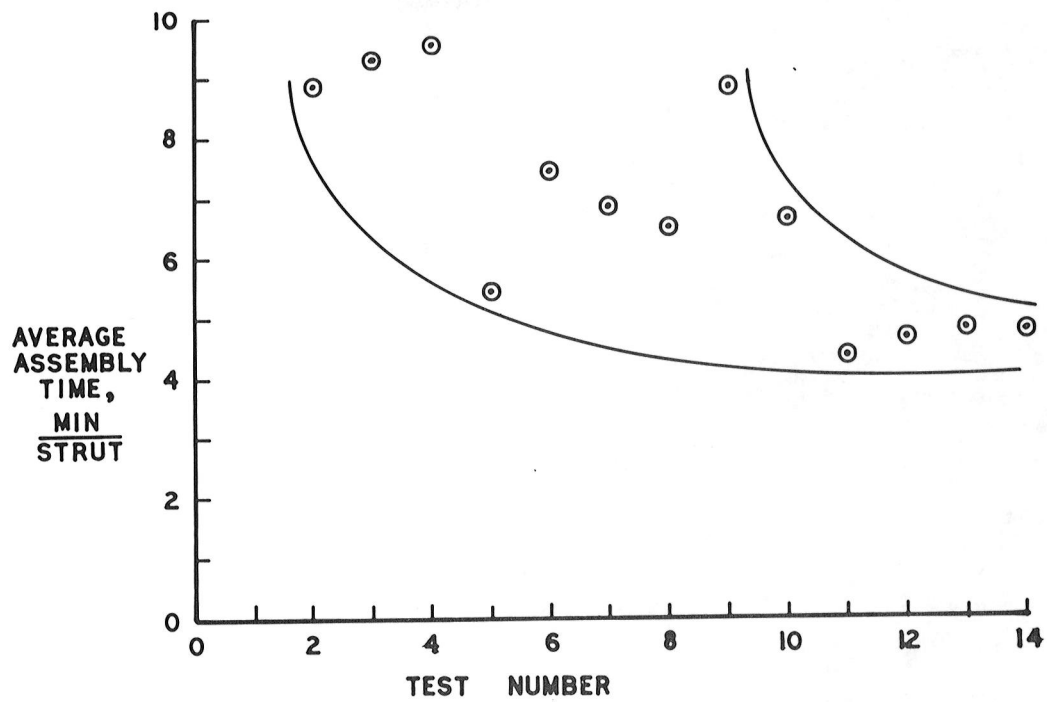


Figure 15. - Average assembly times for unassisted astronaut assembly experiments in Neutral Buoyancy Facility.

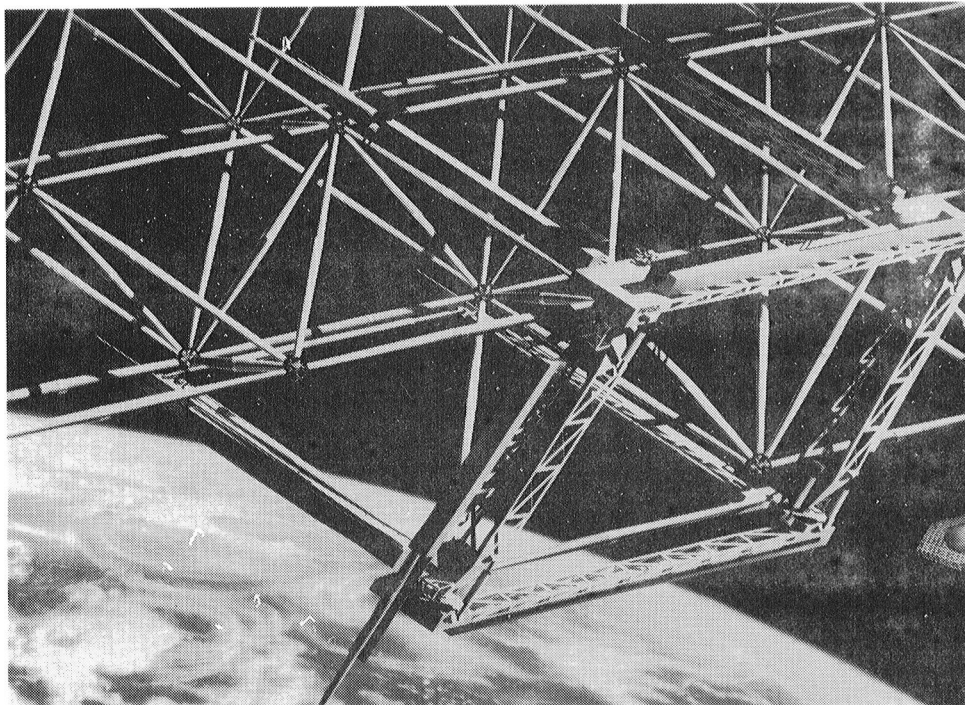


Figure 16. - Automated Assembler (Shuttle free mode) constructing large tetrahedral truss platform.

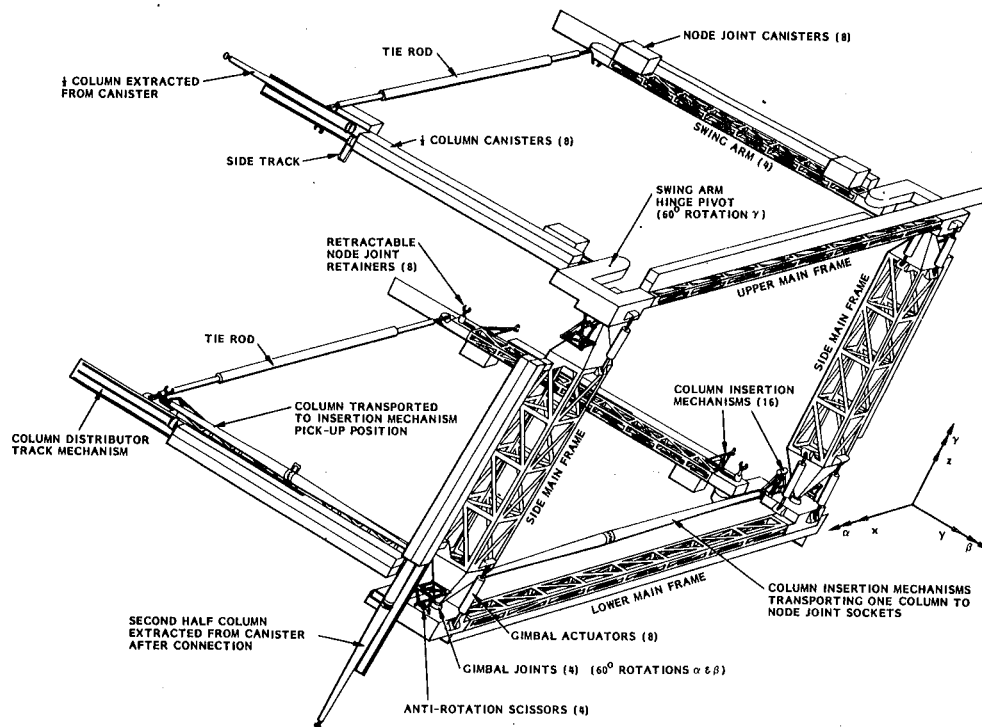


Figure 17. - Detailed schematic of automated assembly machine.

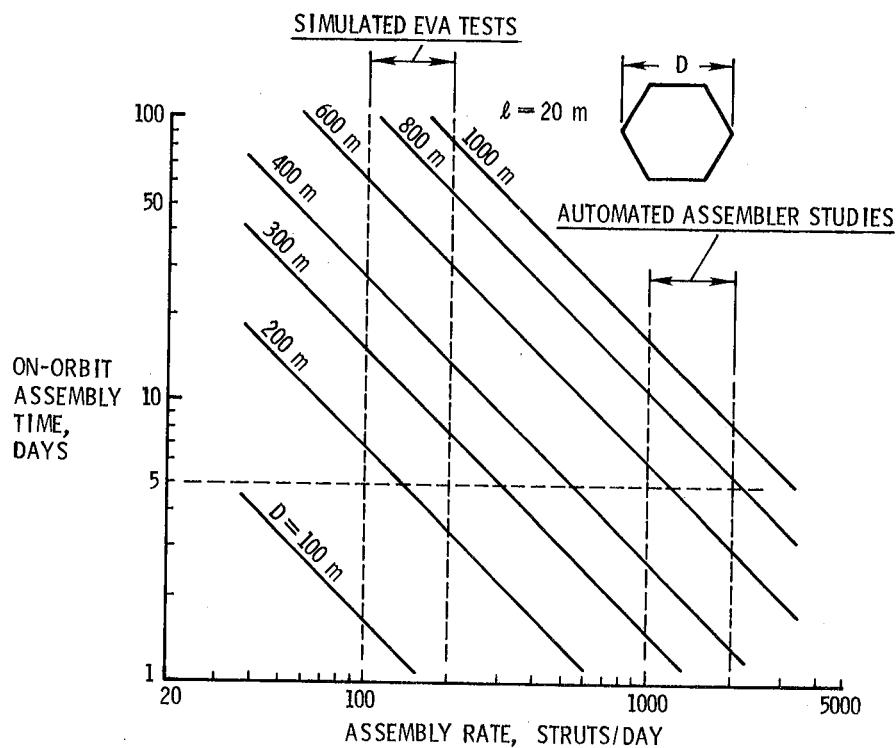


Figure 18. - Current perspective on assembly of erectable structure on-orbit.

1. Report No. NASA TM 81904		2. Government Accession No.		3. Recipient's Catalog No.	
4. Title and Subtitle DEPLOYABLE AND ERECTABLE CONCEPTS FOR LARGE SPACECRAFT				5. Report Date Oct. 1980	
				6. Performing Organization Code	
7. Author(s) H. G. Bush, W. L. Heard, Jr., J. E. Walz, and J. J. Rehder				8. Performing Organization Report No.	
9. Performing Organization Name and Address NASA - Langley Research Center Hampton, VA 23665				10. Work Unit No. 506-53-43-01	
				11. Contract or Grant No.	
12. Sponsoring Agency Name and Address National Aeronautics and Space Administration Washington, D. C. 20546				13. Type of Report and Period Covered Technical Memorandum	
				14. Sponsoring Agency Code	
15. Supplementary Notes SAWE Paper No. 1374, presented at the 39th Annual Conference of the Society of Allied Weight Engineers, Inc. St. Louis, MO., May 12-14, 1980.					
16. Abstract <p>Computerized structural sizing techniques are used to determine structural proportions of minimum mass tetrahedral truss platforms designed for low earth and geosynchronous orbit. Optimum (minimum mass) deployable and erectable, hexagonal shaped spacecraft are sized to satisfy multiple design requirements for: 1) packaging constraints imposed by Space Shuttle limits, 2) fundamental vibration frequencies of the platform and struts, 3) strut axial stiffness reduction due to curvature and/or taper, 4) strut buckling due to design loads such as gravity gradient control, orbital transfer, or assembly, and 5) geometric constraints on strut thickness, diameter and length. Strut dimensions characterizing minimum mass designs are found to be significantly more slender than those conventionally used for structural applications. Comparison studies show that mass characteristics of deployable and erectable platforms are approximately equal and that the Shuttle flights required by deployable trusses become excessive above certain critical stiffness values. Recent investigations of erectable strut assembly are reviewed. Initial erectable structure assembly experiments show that a pair of astronauts can achieve EVA assembly times of 2-5 min/strut and studies indicate that an automated assembler can achieve times of less than 1 min/strut for around the clock operation.</p>					
17. Key Words (Suggested by Author(s)) large space structures, space platforms, deployable space platforms, erectable space platforms			18. Distribution Statement Unclassified -- Unlimited Subject Category 39		
19. Security Classif. (of this report) unclassified	20. Security Classif. (of this page) unclassified	21. No. of Pages 22	22. Price* A02		

